Chem Soc Rev

RSC Publishing

TUTORIAL REVIEW

View Article Online
View Journal | View Issue

Mesoporosity – a new dimension for zeolites†

Cite this: *Chem. Soc. Rev.*, 2013, **42**, 3689

Karin Möller* and Thomas Bein

Received 29th November 2012

DOI: 10.1039/c3cs35488a

www.rsc.org/csr

Frameworks of precisely defined pores with diameters matching the size of small molecules endow crystalline zeolites with valuable size- and shape-selectivity. Being important selective adsorbers and separators, zeolites are also indispensable as solid acids in size-selective catalysis. However, despite being extremely beneficial, micropores impose restrictions on the mass transport of reactants, especially when bulky molecules are involved. The prospect to boost the catalytic power of zeolites and to extend their applications into new areas has prompted numerous efforts to synthesize mesoporous zeolitic materials that combine diffusional pathways on two different size scales. Our tutorial review will introduce the reader to this exciting recent development in zeolite science. We will give a general overview of the diverse strategies on how to implement a secondary pore system in zeolites. We will distinguish top-down from bottom-up and template-assisted from 'template-free' procedures. Advantages and limitations of the different methods will also be addressed.

Key learning points
Short introduction to the field of zeolites
Benefits of hierarchical zeolites
Differentiation of synthesis strategies for mesoporous zeolites
Assessment of pros and cons of synthetic routes

Published on 04 March 2013.

1. How do zeolites relate to mesoporous materials

The tremendous success story of zeolites is based on their broad spectrum of applications in oil refining, as ion-exchangers, in sorption and separation processes, and as size and shape-selective heterogeneous catalysts, as well as their use as encapsulators or slow-release agents. Today, they represent widely used heterogeneous catalysts in chemical industry due to their extraordinary properties such as physical and chemical stability, tunability of pore size and surface properties such as their acidity. Therefore, an enhancement of the functionality of zeolites is expected to have a significant economic impact. This explains the intensive efforts over the last decade to add literally another dimension to zeolites by implementing a mesoporous network into these microporous solids. Zeolites are low-density, crystalline aluminosilicates with interconnected micropores that display an extremely narrow pore-size distribution.

Department of Chemistry and Center for NanoScience, University of Munich (LMU), Butenandtstr. 5-13 (E), 81377 Munich, Germany.
E-mail: Karin.Moeller@cup.uni-muenchen.de, bein@lmu.de;
Fax: +49-89-2180-77622; Tel: +49-89-2180-77805
† Part of the mesoporous materials themed issue.

The traditional labeling of zeolites as 'molecular sieves' depicts, in an illustrative way, one of the major properties of zeolites as being size-discriminating at a molecular level, which is based on their small pore sizes. While a large number of zeolite sieves with varying (small) pore-sizes are available, bulky molecules with sizes larger than about 1 nm are excluded from the internal zeolite surface. Thus bulky molecules can only be catalytically converted utilizing the outer surfaces of the zeolite crystals. For this reason it would be highly desirable to increase the extent of the accessible zeolite surface. Moreover, even if the reactants are small enough to enter the zeolitic micropores, their slow mass transport could be significantly enhanced if their diffusion in the microporous domain is limited to only a few tens of nanometers. Furthermore, a slow mass transport to and away from the catalytic center can increase the possibility of secondary reactions, with coke formation and catalyst deactivation as a consequence. Suitable materials to overcome these limitations should then at best contain all advantages of the microporous zeolites while offering additional diffusion pathways of a larger size as depicted schematically in Fig. 1. But how can zeolites be transformed into mesoporous materials without sacrificing their valued properties of selectivity and catalytic activity?

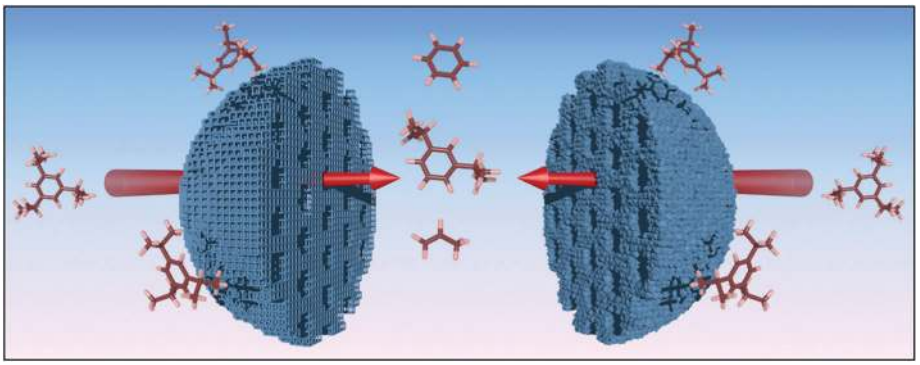

Fig. 1 Schematic representation of a secondary pore system to facilitate the access to and diffusion of bulky molecules within microporous zeolites. These mesopores can be constructed as intracrystalline voids within zeolite single crystals (left) or may be formed as intercrystalline pores in nanozeolite aggregates (right).

The enormous diversity of crystallographically distinct zeolite framework types is documented in the database of the International Zeolite Association.[1] Over 200 different crystalline aluminosilicates or -phosphates have been synthesized since the ground-breaking research performed by Richard M. Barrer about 60 years ago, and several new structures are added every year. Based on the specific connectivity of their corner-sharing tetrahedral TO_4 building blocks (T = Si, Al, P, others), zeolites form three-dimensional extended lattices that are perforated by microporous channels or cavities of various sizes and shapes. Synthetically this is realized with the aid of templates (also called structure directing agents, SDA), either in the form of charge balancing hydrated cations or small organic molecules. The pore sizes of zeolites range between 0.3 and about 1.0 nm in the group of aluminosilicates and extend to about 1.4 nm in the respective phosphates. Each type of zeolite has a unique topology and is classified by a three-letter code. Zeolite structures can be described by the specific secondary building units that are necessary for constructing the three-dimensional framework (such as the sodalite cage that results in LTA when connected *via* double-4-rings, Fig. 2). Moreover, they can be characterized by the dimensionality of the pore network, which can be one-, two-, or three-dimensional depending upon the interconnectivity, and by the pore-size, which is defined by a characteristic number of TO_4 elements (usually 8, 10, 12 for small, medium and large pore aluminosilicates or up to about 24 TO_4 elements for phosphates, respectively). One framework type may be realized by a number of zeolite structures having

Karin Möller

Karin Möller received her PhD in 1984 from the University of Bremen in Germany, working on chemical oscillations on zeolite-encapsulated palladium particles. She spent her post doc years in the USA at the University of Delaware and at the Central Research Department of the DuPont Chemical Company in Delaware and continued as a Research Fellow at the University of New Mexico (Albuquerque) and Purdue University (West Lafayette, IN), focusing on EXAFS spectroscopy for the analysis of small metal or semiconductor particles as well as organometallic complexes encapsulated in zeolites. Her main research interests are focused on the synthesis of zeolites and mesoporous silica materials with new functionalities. Topics include porous silica composites, the synthesis of nano-zeolites and mesoporous silica nanoparticles and their functionalization, high-throughput zeolite synthesis, and the preparation of mesoporous zeolites with tunable secondary pores. Currently she works as a Research Associate at the University of Munich (LMU).

Thomas Bein

Thomas Bein studied chemistry at the University of Hamburg (Germany). He carried out a joint PhD program at the University of Hamburg and the Catholic University of Leuven (Belgium) in the field of zeolite inclusion chemistry and heterogeneous catalysis. After completing an appointment as Visiting Scientist at the DuPont Central Research and Development Department in Wilmington (DE, USA), he built an independent research program as Assistant Professor at the University of New Mexico (USA). Subsequently he was appointed Associate Professor of Chemistry at Purdue University in West Lafayette (IN, USA), followed by promotion to Full Professor of Chemistry at the same university. In 1999 Professor Bein assumed a position as Chair of Physical Chemistry at the Ludwig-Maximilians University in Munich, Germany. Professor Bein's research focuses on the synthesis and function of porous nanostructures such as mesoporous materials, metal–organic frameworks and zeolites, the physical chemistry of interfaces, chemical sensors, targeted drug delivery, and energy conversion.

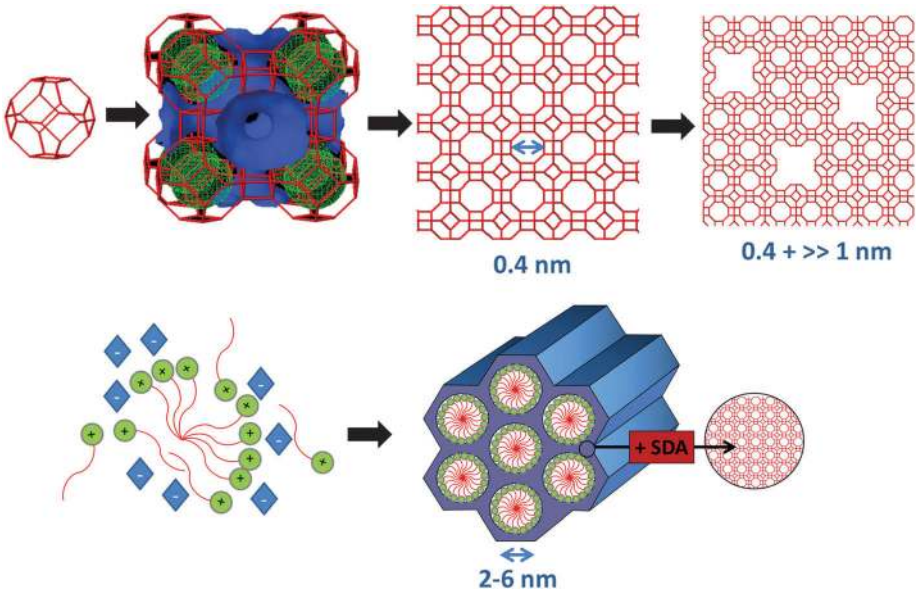

Fig. 2 Constructing mesoporous zeolites. (top) Introducing mesopores into a zeolitic framework: sodalite or β-cages are connected in a cubic array *via* double-four-rings to form the small-pore zeolite LTA. The inner α-cages with a diameter of 1.14 nm are only accessible through 8-ring windows, defining a pore size of 0.4 nm. The introduction of mesopores into the zeolite lattice results in the desired dual pore system for faster diffusion of larger molecules. (bottom) Negatively charged silica oligomers and positively charged surfactant molecules self-assemble into amorphous mesoporous silicas with pores at the mesoscale. A ''zeolitization'' of the amorphous walls would ideally result in mesoporous zeolitic materials.

different chemical compositions. The ratio of the main elements such as Si, Al or P is usually variable to a certain degree and can specifically be altered by inclusion of other (catalytically active) elements such as V, Ti, Ga, Ge, B and others. The framework composition determines if a charge imbalance exists which has to be compensated by a stoichiometric amount of extra-framework cations. These synthesis-based cations can be exchanged with many other cations, including protons, which renders zeolites valuable ion-exchangers as well as solid acids. This extreme flexibility in structure and composition gives rise to tunable chemical and physical properties even within one structure type. Their microporous, crystalline nature makes zeolites highly selective at a molecular level and their low-density framework endows them with large surface areas (between about 300 to 800 $m^2\ g^{-1}$). These tunable properties are the reason for the tremendous success of zeolites in industrial applications such as oil-refining, heterogeneous catalysis, sorption, ion-exchange and separation.

Extending the applications of zeolites to bulkier molecules has long been a driving force for research aimed at the synthesis of large-pore zeolites.[2] A number of new structures with more than 12 T atoms in their pore-determining rings were synthesized by using ever more complex structure-directing templates. Major achievements have been possible especially in the class of phosphates with VPI-5 as the breakthrough representative having 18-membered rings with 1.2 nm pore openings. Newer microporous phosphates with even larger pores have been synthesized, and the recent discovery of the silicogermanate ITQ-43 represents the first example of a truly hierarchical zeolite with interconnecting pores of about 2 and 0.6 nm.[3] However, the lack of chemical and thermal stability as well as the high cost of synthesis of these complex zeolites often limits their application.

The creative exploration of novel template systems has resulted in the discovery of truly mesoporous silica and other materials (see Fig. 2).[4] Here, amphiphilic surfactants or block-copolymers self-assemble into mesoscale aggregates with hexagonal, cubic or disordered morphologies in the presence of silica (or other oxide) precursors and direct the silica condensation in the hydrophilic region of the aggregates. Accessible mesopores confined by an amorphous silica shell are obtained after removing the micellar templates by calcination. Pore sizes are tunable over a large range between 2 to more than 60 nm, depending upon the surfactant (and optional swelling agents) used. These micelle-templated silica (MTS) materials seem to be ideal precursors for creating hierarchical zeolites by transforming the amorphous wall structure into microporous crystalline zeolites, a process referred to as ''zeolitization''. This goal was approached in two different ways by exploiting a dual templating route. The direct approach combines the micropore-forming template (SDA) or alternatively pre-made zeolitic nanoclusters (seeds) with the reaction mixture of the MTS materials, containing its structure-directing supramolecular template. On the other hand, secondary reactions can be performed by impregnating the premade mesoporous materials with the zeolite SDA or zeolite seeds, followed by hydrothermal conversion.[5] However, these attempts to crystallize the amorphous wall structure have generally resulted in phase-separated composites with microporous and mesoporous domains. Apparently there is a mismatch between appropriate zeolite synthesis conditions and those for mesoporous oxides with amorphous walls. Even though the creation of zeolite domains

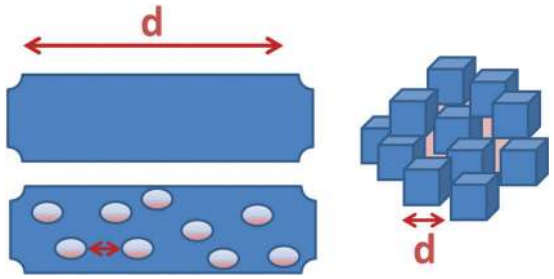

Fig. 3 Increasing the external surface area and reducing the diffusion distance *d* by either incorporating a secondary pore system into large zeolite crystals or by reducing the crystal dimensions to the nanosize in zeolite aggregates.

in such materials can drastically improve the thermal stability or acidity when compared to the amorphous mesoporous materials, the strong acidity and catalytic activity of zeolites are still unsurpassed. To generate completely crystalline microporous/mesoporous zeolites, it seems more promising to start from well-explored zeolite synthesis procedures and to adopt additional means to impose mesoporosity.

Two major goals can be accomplished when mesopores are added to the microporous framework of zeolites:

a) enabling the processing of molecules that exceed the size of zeolite micropores

b) building channels for faster diffusion and mass transport to and away from the catalytic centers in order to accelerate catalytic conversions avoids unwanted secondary reactions and coke formation.

The zeolite surface area can be described as the sum of its internal and external surface areas, the first exclusively formed by the inherent micropores, the latter by the remaining external surface area, including meso- and macropores. To aid the conversion of larger molecules as indicated in the first goal primarily requires better access of these reactants to the external surface of the zeolite phase since the internal surface remains out of reach. A gain in conversion is thus directly related to an increase in zeolite external surface area and its exposed acid sites. Maximizing the external surface area can be achieved in two ways: either by implementing a secondary mesopore network into zeolite single crystals or by reducing the individual crystallite size from the micrometer to the nanometer scale, thus creating intercrystalline mesopores. Both concepts lead to the exposure of a larger fraction of the well-defined, stable (and possibly highly acidic) zeolite surface for adsorption and conversion of bulky reactants. Simultaneously, if a catalytic degradation or isomerization of bulky reactants into smaller reaction products occurs at the external surface, these products can venture into the interior of the zeolite domains. Hence, one can further utilize catalytic activity in the micropores as well as additional molecular sieving effects, if so desired.

Creating a larger external surface area simultaneously reduces the diffusion distance ***d*** in the microporous phase; this holds for both mesopore-containing single crystals and intergrown small zeolite nanocrystals, as demonstrated in Fig. 3. Naturally, enhancing mass transport is not only relevant for new applications with bulky reactants but also for transport-limited reactions traditionally performed with zeolites. Hence, mesopores *literally* add another dimension to the already highly valued catalytic capabilities of zeolites.

2. General strategies to create mesoporosity in microporous zeolites

The last decade has brought about a number of different strategies to accomplish the synthesis of zeolites with additional mesoporosity, and several excellent reviews report on the advances made in this field.[6] Concerning hierarchical materials prepared *via* multi-step replication of mesoporous scaffolds or zeolites featuring additional macropores, we refer to a very recent article.[7] In this tutorial review we will highlight the major strategies that create truly zeolitic mesoporous materials. A comprehensive account on mesoporous zeolitic materials can be found elsewhere.[8]

Principally we can distinguish synthesis strategies that (a) use a dual templating route, including the common zeolite structure directing agents and additionally a secondary template for mesostructuring the zeolite crystals, (b) use only a single but multifunctional template, containing structure directing fragments for the micro- and mesoscale in the same molecule, (c) rely on reaction conditions that make secondary templates unnecessary and (d) use leaching reactions performed on pre-made zeolites.

The dual-templating route (a) follows the same principal idea that has been proven to be so successful in zeolite synthesis at the microporous scale: finding a sacrificial scaffold for the mesoscale that directs the zeolite growth without becoming an integral part of the zeolite framework during crystallization and that can be removed without loss of the final structural features. Here we can distinguish different secondary templates by their physicochemical nature and divide them roughly into 'hard' or 'soft' templates, being of more or less rigid nature. Soft templates can again be divided into macromolecular polymers, amphiphilic surfactant derivatives or large silylating agents. A structural ordering of the secondary pores comparable to the periodic mesoporous silica materials is usually not achieved unless a replication mechanism of ordered scaffolds is involved. Using multifunctional templates (b) is aimed at achieving just this ordering of micro- and mesopores at the same time through the action of a single, however complex, templating molecule. The third approach (c) intends to simplify the synthetic requirements and to save additional cost by stimulating the growth of nanozeolite aggregates that self-assemble into a mesoporous network. These first three strategies are also frequently addressed as 'bottom-up' procedures in contrast to the last category (d). This is regarded as a 'top-down' method because mesopores are etched into a pre-existing zeolite matrix. A simplified graphical sketch of these different mesostructuring approaches is given in Fig. 4.

It should be noted that principally two different kinds of mesopores might arise depending on the choice of template or

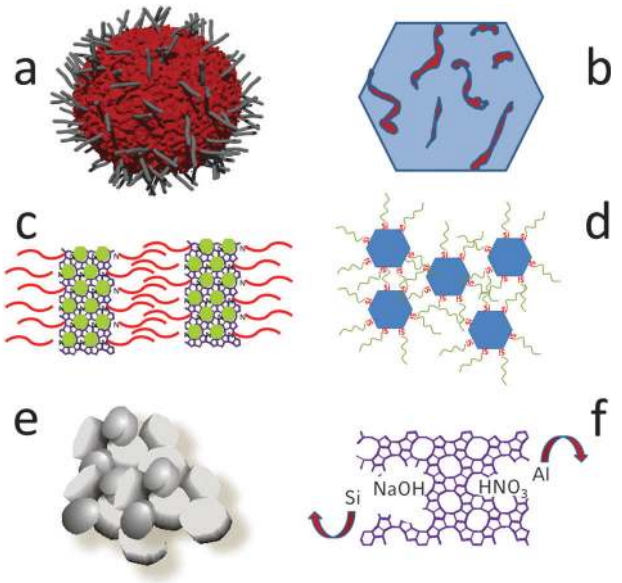

Fig. 4 Overview of different strategies to implement mesoporosity in microporous zeolites: (a) inclusion of a secondary hard template in form of rigid fibers, (b) incorporation of a secondary soft template, (c) application of a bifunctional template for micro-and mesostructuring, (d) covalent bonding of organosilane spacers to zeolite seeds, (e) formation of nanoparticle aggregates without secondary templates, (f) post-synthetic leaching of alumina or silica species from premade zeolites.

Published on 04 March 2013.

reaction conditions. Hard templates are usually intended to create *intracrystalline* mesoporosity, leaving a negative imprint of their morphology in single crystal zeolites after removal by calcination. In some instances, intrazeolite mesostructuring can also be generated by polymeric aggregates. The products are in the true sense hierarchical zeolites, embodying interconnected micropores and mesopores in the same particle. However, depending on the size of the template particles or their chemical affinity towards the zeolite gel either intrazeolite or *interzeolite* mesopores might be induced, the latter resulting from the formation and aggregation of nanozeolites. Interparticle mesopores can be formed as an inherent materials property within partially condensed/sintered nanoparticle assemblies as opposed to the (transient) textural mesopores formed from simple packing of individual nanozeolites.

In our discussion about the various pathways towards mesoporous zeolites we will describe the general synthetic aspects of the different approaches, their versatility with respect to zeolite structures, the effect on attainable pore sizes, tunability and yield and will reflect on the complexity and efficiency of the procedures.

3. Bottom-up zeolite synthesis by dual templating on the micro- and mesoporous length scale

The bottom-up synthesis of mesoporous zeolites is mostly performed using the common hydrothermal zeolite synthesis procedures and in some instances *via* a steam-assisted conversion treatment (SAC; see below). However, instead of relying only on the templating action of a molecular structure directing agent (SDA) responsible for micropore formation, a second larger template is added in order to create the desired mesopores.

3.1 "Hard" scaffolds as secondary template: carbon

Adding a hard template to the synthesis gels of zeolites is generally a straightforward and versatile procedure. Resulting in physical mixtures with the zeolite gels, this route seems to be applicable to a broad range of zeolite as well as metallophosphate synthesis procedures. Hard templates can consist of different materials such as metal-oxide nanoparticles, plant materials, resin beads or aerogels, but carbon compounds have been used most frequently. Here, the group of Jacobsen has performed most of the pioneering work using commercial carbon Black Pearls (BP 2000 or BP 700, particles with 12 or 18 nm diameter, respectively), porous carbons (Mogul L or Monarch 1300, pore diameter 30 and 10 nm, respectively) or carbon fibers (CNF, 20–40 nm diameter).[9] The carbon powders or compressed carbon pellets were originally intended to assist the synthesis of nanozeolites with controlled particle size. For this purpose zeolites were crystallized in the confined space between the carbon particles or within the pre-formed pores of the porous carbons. Completely soluble zeolite precursors were therefore used to successively impregnate the carbon matrix just enough for zeolite growth to occur exclusively within the small carbon pores. Retrieval of these composites by filtration, the decomposition of the micropore template under nitrogen at 550 °C and the proton ion-exchange was easily performed and when the carbon matrix was finally removed by calcination in air, powders of acidic ZSM-5 with very small (about 20 nm) nanoparticle domains were obtained. In contrast, when an excess of zeolite precursor solution was used in the impregnating process, crystallization occurred all around the carbon particles, resulting in mesoporous zeolite single crystals with 5 to 50 nm pores instead (see Fig. 5a).

This approach has been used mainly for the synthesis of MFI-type zeolites, including the aluminosilicate ZSM-5, the highly siliceous form silicalite-1 and the titanium form TS-1 as well as the corresponding MEL-type zeolites (ZSM-11).[10] Additional zeolite types and aluminophosphates, such as BEA (beta), AFI ($AlPO_4$-5) and CHA ($AlPO_4$-34) were prepared as mesoporous single crystals *via* the hydrothermal fluoride route.[11] The fluoride ion is used as mineralizer here in contrast to the OH^- ion in the more common alkaline synthesis route, allowing one to work at a low pH around 5 that favors a slow growth and the formation of single crystals. In this way even large (micron-sized) single crystal beta was obtained, which normally exists in the form of much smaller crystallites. The size of the mesoporous single crystals or single crystal-like aggregates is usually at least 1 micron when using carbon powders as sacrificial templates.

Challenging problems frequently encountered with carbon templates are inhomogeneous mixtures of mesoporous zeolites with solely microporous single crystals or nanozeolites as well

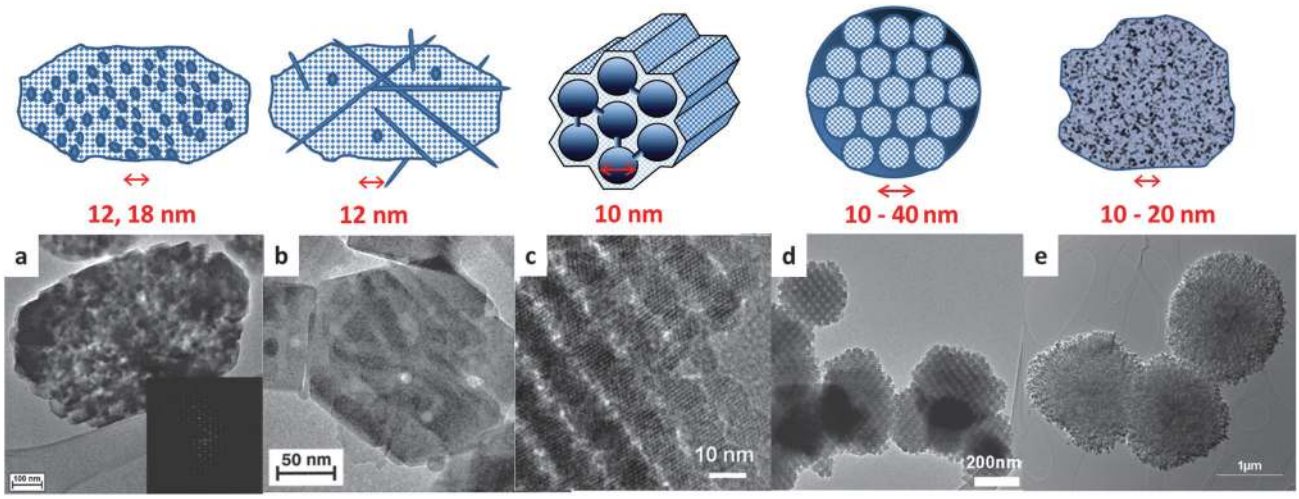

Fig. 5 Overview of hard templating strategies using carbon. Top: graphical sketches of zeolite-carbon composites, bottom: electron micrographs of final mesoporous zeolite products. (a) Single crystal of ZSM-5 made with 12 or 18 nm carbon pearls, including the respective electron diffraction, (b) silicalite-1 single crystals made with about 12 nm wide, micron-sized carbon nanotubes, (c) ordered mesoporous silicalite-1 made with KIT-6 silica replicated CMK-L carbon; micropores and mesopores are visible, (d) three dimensionally ordered mesoporous beta made from 3DOm carbon replicas, (e) mesoporous zeolite ZSM-5 generated with pyrolyzed sugar/silica composites. Adapted with permission from (a) copyright 2000, American Chemical Society,[9] (b) copyright 2001, American Chemical Society,[13] (c) copyright 2012, Elsevier,[15] (d) copyright 2011, American Chemical Society,[17] (e) copyright 2007, American Chemical Society.[18]

as the formation of inaccessible mesopores through the complete occlusion of individual carbon particles. To avoid a phase separation between the hydrophobic template and the hydrophilic zeolite gel, crystallization of the impregnated carbon matrices is often performed *via* the "steam-assisted-conversion" or SAC method. Here, in contrast to the common hydrothermal conversion, the precursor gel is dried and kept apart from an aqueous phase in the bottom of the autoclave. The gel is thus only exposed to saturated steam.

Mesopore sizes in carbon-templated zeolites range from about 10 to 50 nm and the size distribution is generally relatively broad. Other carbon sources were therefore tested to create more defined mesoporous imprints and to further allow a better control of the crystallization conditions. Alternative materials include carbon aerogels, carbon nanotubes, ordered carbon nanotubes or even graphene oxide sheets.[7]

Monolithic aerogels can serve as precursors to fabricate carbon aerogel bodies with interconnected pores and variable pore sizes. The aerogels are easily prepared by polymerization of resorcinol–formaldehyde gels which are then dried under supercritical conditions with CO_2. Highly porous aerogels result that are subsequently pyrolyzed to give the respective porous carbon skeletons. The mesopore size in these carbons can be tuned by the reaction conditions; for instance in one study 23 nm mesopores were formed, separated by carbon walls with a thickness of about 10 nm.[12] These bodies are then immersed in so-called "clear solutions" of highly diluted, molecular zeolite precursors and are hydrothermally converted into zeolite/carbon composites. Zeolite intergrowth in these three-dimensional pore networks stabilizes the porous zeolite replicas after removal of the carbon scaffold by calcination. In this way, mesoporous zeolites ZSM-5, A and Y were obtained with narrow pore-size distributions reflecting the thickness of the carbon walls.

Structurally even more defined but higher priced single or multiwalled carbon nanotubes or the more cost-effective versions of carbon nano-fibers were used to create unidirectional mesopores that ideally penetrate the single crystals completely. For instance, silicalite-1 crystals with about 20 nm wide straight channels were prepared by sequential impregnation of long, micron-sized carbon fibers (see Fig. 5b).[13] Even narrow, slit-like pores could be created using single sheets of graphene oxide. This hydrophilic carbon scaffold presumably initiated silicalite-1 nucleation along the carbon layers, forming either electrically conductive composites or the respective mesoporous zeolites with 2–2.5 nm pores after calcination.[14]

Another aspect of mesopore design is not only to create evenly sized pores, but to also arrange these pores into an ordered secondary pore system. Highly ordered mesoporous carbon scaffolds (CMK-1 or CMK-3) were prepared for this purpose by replication of MCM-48 or SBA-15 mesoporous silicas. First attempts to form mesoporous zeolites by a second replication process using these mesoporous carbons resulted in inhomogeneous silica phases with low surface areas and micropore volumes. It was believed that the pore size of the carbon matrix of 2–3 nm was still too restricted for zeolite nucleation, causing migration of the aqueous precursor gel to the external surface of the hydrophobic templates during hydrothermal conversion. Better results were achieved when the SAC method was used on the CMK/silica composites that still contained the original MCM/SBA precursors as digestible silica source. However, only when large-pore silicas (KIT-6) with a pore diameter of about 10 nm were used for the carbon replication (CMK-L) and when the humidity during the steam conversion was carefully adjusted to 85% was it possible to synthesize highly crystalline silicalite-1 with large surface areas and the typical

micropore volume for this structure type (see Fig. 5c).[15] The size of the final mesopores was found to be about 9 nm.

Ordered meso- to macroporous carbon scaffolds with interconnected mesopores can also be made from colloidal silica imprints. Here, highly defined silica spheres of predetermined diameters between 10 to 40 nm are three-dimensionally packed and impregnated with a carbon precursor that is then polymerized and subsequently carefully pyrolyzed. Removal of the silica spheres by etching with KOH finally results in the inverse opal carbon structures (colloidal imprinted carbons, CIC, or three-dimensionally ordered mesoporous carbons, 3DOm's).[16] Zeolite growth in the confined spaces of these scaffolds has been performed either by the SAC method or by hydrothermal conversion. The latter procedure relies on multiple impregnation/conversion cycles to successively grow the zeolites in the confined space of the carbon scaffolds without causing an uncontrolled growth on the outside. A number of different, three-dimensionally ordered mesoporous zeolites were made in this way, including zeolite beta, FAU, LTA and LTL with highly ordered, tunable mesopores between 3–7 nm (see Fig. 5d).[17] The single crystal growth is believed to start from seeds in single cages followed by propagation to the neighboring voids through the connecting windows in the carbon matrix. Polycrystalline assemblies were observed only for LTL, where abundant nucleation was dominating the crystal growth. A commercial implementation of zeolites prepared in this way is not very likely due to the time-consuming and costly preparation; however, they could serve as excellent model systems for studying fundamental problems such as mass transfer limitations in catalytic applications.

A less ordered but straightforward and inexpensive carbon template can be made *in situ* when sugar-impregnated silica gels are pyrolysed. These intimately mixed carbon/silica precursors are then readily available for use in the hydrothermal zeolite synthesis. Large aggregates of ZSM-5 and ZSM-11 nanoparticles were obtained in this way with tunable pore-sizes between 10 and 20 nm, depending on the sugar/Si ratio chosen (see Fig. 5e).[18]

Other non-carbon templates that are readily available and cost effective include nanosized oxides such as MgO or $CaCO_3$ particles, polystyrene pearls or poly(methyl methacrylate) spheres (PMMA) or even bio-templates such as wood cells or diatoms, all of which usually generate secondary pores on a larger scale in the macro range.[6c]

3.2 "Soft" secondary templates: polymers, silylated surfactants, bifunctional surfactants

These templates are even more versatile in nature than carbon additives and can vary in size and functionality. They share a (macro)molecular character and an inherent flexibility on a relatively short length scale. Soft templates may not only act as a physical scaffold but may in some cases interact chemically with the growing zeolite phase. The largest members of this group are macromolecular structures such as soluble polymers. They are tunable in their chemical composition, molar mass and surface charge. For instance, the cationic polymer polydiallyldimethylammonium chloride (PDDA) was chosen by the group of Xiao as secondary template because of its high charge density in order to prevent any interfacial incompatibility between template and zeolite gel.[19] As discussed above, this effect is sometimes encountered between uncharged, hydrophobic templates such as carbon scaffolds and the negatively charged aluminosilicate gels. By adding the cationic polymer PDDA to a zeolite gel during hydrothermal conversion, mesopores of 5 to 40 nm were created within 300 nm particles of zeolite beta. Since this diameter is similar to the estimated size of the solvated polymer, it was concluded that the pores were created by inclusion of the polymer strands. Tuning of the pore size was also possible over a certain range (between 18 to 25 nm) by simply adding increasing amounts of PDDA during the hydrothermal synthesis.

Imposing even structural ordering of mesopores with "soft" templates is a great challenge. In a study aimed at this challenge, the copolymer polystyrene-*co*-4-polyvinylpyridine (M_W of 10^5) was treated with methyl iodide, thus forming a cationic amphiphilic copolymer. Supposedly supported by its favorable interactions with the negatively charged silica species it was possible to create unidirectional mesopores of 6–60 nm along the *b*-axis within single crystals of ZSM-5 with this polymer.[20] These mesoporous MFI zeolites and a related ZSM-5 made by PDDA templating causing randomly arranged mesopores were then compared in the condensation reaction of bulky substrates. The material with oriented mesopores showed a much higher conversion and it was speculated that a large fraction of the non-oriented mesopores in the PDDA-based reference sample is inaccessibly hidden within the bulk of the zeolites. This high conversion was even comparable to or better than those reported for uni- or multilamellar ZSM-5 made with bifunctional templates (see Section 3.3).

However, polymers might not only create intracrystalline mesopores caused by inclusion, but they can also act indirectly as flocculating agents. This was shown in a dense-gel synthesis of zeolite beta that resulted in colloidal solutions of nanosized beta without addition of the cationic PDDA but that turned into stable mesoporous aggregates under the influence of the polymer.[21] Mesopores were created here from the interstitial voids in the nanoparticle assemblies that were tunable between 40 to 360 nm by changing the polymer concentration.

Amphiphilic, micelle-forming surfactants of low charge-density or non-charged larger block-copolymers are well recognized for the formation of mesoporous amorphous silicates such as MCM-41 or SBA-15 (MTS-materials). The zeolitization of these materials, that is a conversion of the silica walls into crystalline zeolite while keeping its ordered mesostructure intact, was observed to be difficult. It was speculated that this difficulty was caused by the incompatibility of the crystalline zeolite lattice and the micelle curvature, leading to incomplete crystallization or phase separation. However, it turns out that with an obligatory gel pretreatment and a carefully chosen zeolite gel composition it is possible to use the conventional cetyltrimethylammonium (CTAB) surfactant to form completely crystalline mesoporous ZSM-5 aggregates, however only with disordered mesopores.[22] It was argued that the ageing process creates subnanometer zeolite seeds that have a good size-match

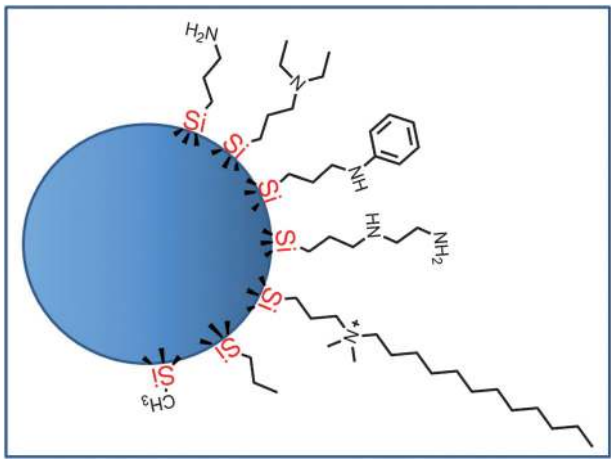

Fig. 6 Representative organosilanes used for covalent attachment onto pre-zeolitic silica particles. From top to bottom: APTMS: 3-aminopropyltrimethoxysilane, DATMS: (*N*,*N*-diethyl-3-aminopropyl)trimethoxysilane, PHAPTMS: phenylaminopropyl trimethoxysilane, TMPED: *N*-[3-(trimethoxysilyl) propyl]ethylenediamine, TPDAC, TPHAC, TPOAB: [3 (trimethoxysilyl)propyl] dodecyl, -hexadecyl, -octadecyldimethylammonium chloride/bromide, PTES: propyl triethoxysilane, MTES: methyl triethoxy silane.

with the micelle morphology and can therefore cooperatively self-assemble into mesoporous zeolites. Other polymers such as polyethylene oxide (PE), propylene oxide (PO), polyvinylbutyral or the block-copolymer F127 or P123 were used as additives, in some instances using a SAC process for generating mainly zeolites of the MFI family, with MEL or BEA structure, as well as for synthesizing mesoporous aluminophosphates. Cost-effective, environmentally friendly hydrophilic carbohydrates in the form of cellulose, starch or sugars were also investigated, showing promising results.[23] We note that an issue encountered with polymer-based zeolite synthesis is frequently a relatively low microporosity when compared to the parent zeolites.

Above we have shown that polymers can impart mesoporosity in zeolite products by either inclusion in zeolite crystals or by assisting in the aggregation of zeolite particles, leading to textural (interparticle) mesoporosity. In order to create more defined pores smaller than 10 nm, the group of Pinnavaia introduced the idea of using multiple-silylated branched polymers to actively structure zeolite morphologies. This size-range was anticipated to be advantageous for catalytic cracking of larger molecules while still imposing selectivity on the products. Forming covalent Si–O–Si linkages with the zeolite precursor promises to minimize any phase separation, and the polymer backbone can be used as spacer between the crystallizing zeolite domains (see Fig. 8a). While the silane fragment is incorporated into the crystalline zeolite body, the organic fraction will be removed by calcination simultaneously with the micropore template. This concept was presented by using polyethyleneimine or polypropylene oxide diamine that was silylated with glycidoxypropyl trimethoxysilane. It was added to the zeolite gel to prepare ZSM-5, and resulted in intracrystalline mesopores of 2–3 nm, where the actual size was slightly dependent on the molecular weight of the polymer.[24]

A related concept is based on using not polymeric but monomeric silylated templates in the form of terminally siloxy-functionalized alkyl chains as secondary templates. Anchoring only the silylated end to the zeolitic phase leaves the remaining alkyl residue to control the mesopore dimensions. Variation of the length and composition of this alkyl fragment offers the possibility to create a large range of custom-made hierarchical zeolites. A number of alkylated siloxanes with different degrees of complexity have already been studied, very much stimulated by the work of Serrano and Ryoo. These chemically reactive templates can be classified into three different groups: (a) cationic silylated surfactants, (b) neutral alkyl amino siloxanes and (c) simple alkylated siloxanes (see Fig. 6).

Cationic organosilanes are modeled after the amphiphilic templates used for the synthesis of mesoporous silicates, but are improved through their specific functionality. They are equipped with three important segments: first, a hydrolysable, reactive siloxy group that is able to form covalent bonds with the silica gels. The covalent Si–C bond is strong enough to withstand the usually harsh conditions during the hydrothermal synthesis under basic conditions. Second, they contain one or more quaternary ammonium head groups as potential zeolite structure-directing groups, which also create a hydrophilic character that is compatible with the aqueous zeolite phase. Finally, they have a flexible hydrophobic hydrocarbon tail with adaptable length to fashion the mesopore dimensions. Templates of this group were first synthesized in the group of Ryoo who showed that tailored mesoporous MFI zeolites can be made in this way. Here, the template (3-(trimethoxysilyl propyl))hexadecyl dimethyl ammonium chloride (TPHAC) was added (at a few mol% of the total silica content) directly to the common MFI synthesis gel that was then hydrothermally converted.[25] Depending on the respective alkyl chain length, which was varied between C_{12} to C_{18} and the reaction temperature, disordered mesopores of about 2 to 7 nm were formed (see Fig. 7). Similarly, zeolite LTA with 10 nm mesopores was made, displaying a polycrystalline cubic morphology.

Besides zeolites of the MFI group, faujasite (FAU) is a very important structure that is heavily used in industry in catalysis and catalytic cracking for gasoline production. Mesopores of 18 nm were created successfully in zeolite Y, a faujasite with a medium Si/Al ratio, with the octadecyl derivative TPOAB ($[(C_2H_5O)_3SiC_3H_6N(CH_3)_2–C_{18}H_{37}]Br$), and even zeolite X was recently constructed with 7 nm pores using TPHAC. Zeolite X is the high aluminum version of FAU (Si/Al ratio 1.0–1.5) that is not easily transformed into mesoporous faujasite using the commonly applied desilication route (see Section 5.2). Using the organosilane route resulted in micron-sized zeolite X with a complex architecture of nanosheets that are assembled like a house of cards and create a three-fold pore structure with micro-, meso- and macropores of 0.74, 7 and 200 nm, respectively.[26] An external or mesopore surface area (obtained from the total surface area minus the micropore surface area) of 130 $m^2\ g^{-1}$ as compared to 11 $m^2\ g^{-1}$ in a reference sample was created as reactive surface for bulky molecules.

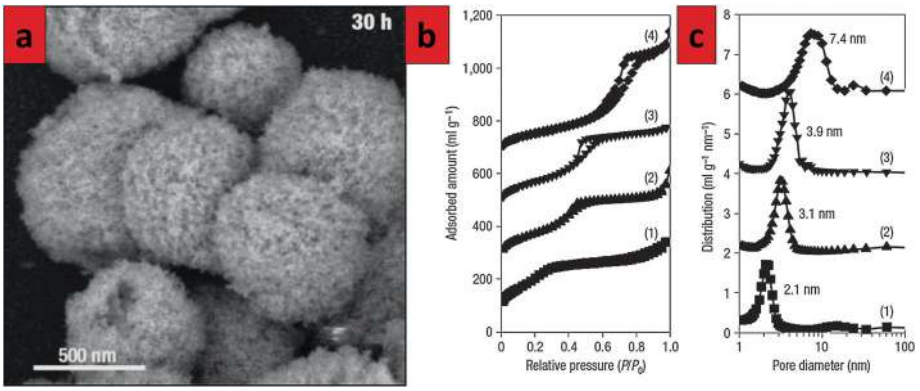

Fig. 7 Mesoporous zeolite MFI made with cationic silylated surfactants with different chain length C_{12}, C_{16}, C_{18} (TPDAC, TPHAC, TPOAB). (a) The SEM shows the sponge-like surface of the polycrystalline MFI, (b) N_2 sorption isotherms document two distinct sorption steps, at very low and medium relative pressure, indicating the coexistence of micropores and mesopores and (c) the corresponding pore size distributions (BJH) reflect the tunability of the pore diameters; sample 4 was made with TPHAC at a higher reaction temperature. Adapted by permission from Macmillan Publishers Ltd: (Nature Materials) from ref. 25, copyright (2006).

This class of templates was used with a number of MFI-type zeolites including TS-1 and Fe-ZSM-5, which were then tested in different catalytic reactions involving large molecules such as benzaldehyde condensation reactions or smaller molecules such as the selective hydroxylation of benzene to phenol. For instance, mesoporous MFI showed a higher activity towards larger molecules compared to their common microporous counterparts. Interestingly, when the mesoporous zeolites were treated with a dealuminating step that predominantly removed the aluminum from the external surface, the activity was almost lost. Catalysis with small molecules that were able to penetrate the micropore system was unaffected by this treatment. It was concluded that the catalytic conversion of the bulky molecules occurs mainly at the pore mouth of the newly created external surface.[27] However, when the hydroxylation of benzene to phenol was performed with mesoporous Fe–ZSM-5 it was nearly four times more active than the best, optimized steam-calcined Fe–ZSM-5.[28] In this case the often-observed extended activity can be explained by a high resistivity against deactivation by coke. The polyaromatic side-products are adsorbed on the large external surface, leaving the microporous domains longer unaffected. This nicely demonstrates the benefit of mesoporous zeolites for whole new classes of catalytic reactions as well as for established procedures. New opportunities for applications also include the surface-functionalization of mesoporous zeolites that is possible on their large external surface. For example, this was demonstrated with oxoiminopropyl triethoxysilane on calcined mesoporous ZSM-5. The attached ligand was used for palladium complexation, thus creating a new catalytic platform.[29]

Tunability of the mesopores is a highly desirable property in order to add versatility to the hierarchical zeolites. It was shown that this is possible not only by extending the length of the hydrophobic tail in the TPHAC template, but also by just adding higher concentrations of the same surfactant. It appears that this template acts as its own pore extension agent by incorporating excess molecules into the micelles of the covalently bonded bilayer. An extension to even 24 nm pore diameter was observed when the synthesis gel was enriched with the triblock copolymer $EO_{20}PO_{70}EO_{20}$ (P123) (see Fig. 8b). Xe diffusion occurred 200 times faster in mesoporous LTA prepared by this route compared to solely microporous LTA.[30]

Neutral, commercially available organosilanes were studied by the group of Serrano. They used a multiple-step synthesis

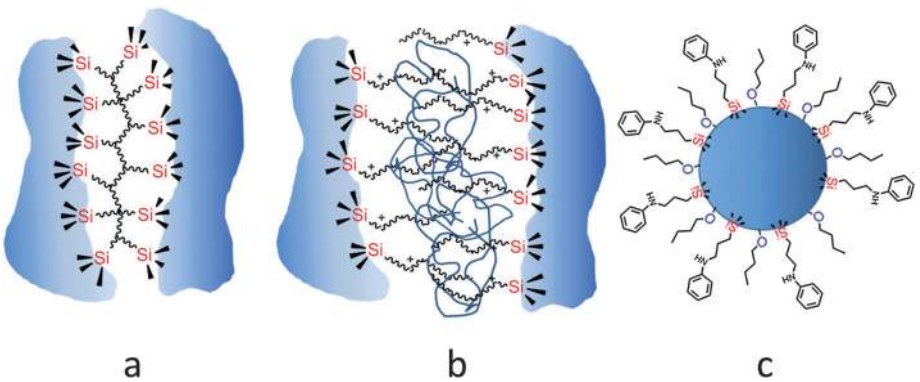

Fig. 8 Covalent silylation of (a) zeolite precursors with a multi-functionalized silylated polymer, (b) the precursor gel with a cationic amphiphilic surfactant in the presence of a block-copolymer as pore extender, and (c) silylation of preformed seeds with a neutral organosilane and an auxiliary alcohol acting as pore extender.

route to perturb zeolite growth through seed silanization. In order to prevent the possible inclusion of the organosilanes in the micropores of zeolites during synthesis, they preconditioned the zeolite gel, allowing the formation of zeolite seeds. Usually a three-step procedure is applied: (i) zeolite seeds are first formed by refluxing the zeolite gel at 90 °C, (ii) functionalization of the seeds is performed by a second reflux with organosilanes such as phenylaminopropyl trimethoxysilane (PHAPTMS), and (iii) final crystallization proceeds under hydrothermal conditions. Zeolites ZSM-5 and beta were made by this procedure and resulted in aggregates of very small nanoparticles with interparticle mesopores.[31] The MFI materials obtained with the methods of Ryoo *et al.* with TPHAC[25] and by Serrano *et al.* as described above are almost identical. Both methods create an exceptionally large total surface area of about 590 m^2 g^{-1} (microporous ZSM-5 usually has about 370 m^2 g^{-1}), a mesopore surface area of about 350 m^2 g^{-1} and mesopore size of about 5 nm, and both lead to the aggregation of very small, about 10 nm sized crystalline nanozeolites. The textural properties of the mesoporous zeolites can also be varied by changing the pre-crystallization conditions, the concentration or the tail group of the organosilane. Larger mesopore volumes and pore sizes were further obtained upon addition of auxiliary alcohols like 2-propanol or methanol. This leads to a decrease in gel viscosity and presumably increases the silanization degree of the nanozeolites. Additionally it allows for an alkoxylation of the surface, increasing its hydrophobicity and enhancing the protective layer structure (see Fig. 8c).[32]

A systematic study on the crystallization conditions of mesoporous ZSM-5 using molecular silica and alumina sources (tetraethoxysilane, TEOS and aluminum isopropoxide, IPA) together with PHAPTMS revealed that a preconditioning of the zeolite gel was a prerequisite for crystallization to happen. Crystallization did not occur when the organosilane was added directly to the untreated gel, presumably due to a simultaneous hydrolysis and mutual co-condensation of the different precursors.[33] However, a related study using more simple alkoxysilanes (methyl, -propyl and octyl triethoxysilane, MTES, PTES and OTES, respectively) obtained mesoporous ZSM-5 with very similar morphology, mesoporous surface area as well as secondary pores of similar sizes when the organosilanes were used in a single-step reaction. The concentration of the silanes as well as their hydrophobicity (chain length) did not affect the pore size in this case, but only influenced the size of the aggregated particles.[34]

The concept of mesopore generation through interrupted crystallite growth was very recently adapted to the silicoaluminophosphate SAPO-11. Zeotypes of this AEL framework type have a one-dimensional pore structure that is especially prone to blocking and thus causing transport problems. SAPO-11 is known for its isomerization activity but its small pore size of about 0.4 × 0.65 nm restrains the formation of di-branched isomers and secondary mesopores will very likely augment its mass transfer ability to a great extent. SAPO-11 was therefore synthesized in the presence of a mesopore mediator in the form of alkylphosphonic acid (tetradecylphosphonic acid, TDPA) in a one-step reaction that generated large 4–6 μm pseudospherical aggregates with a markedly increased surface area. The TDPA modifier had apparently donated the P atoms as framework-terminating elements and generated additional intracrystalline mesopores of 5 nm by virtue of its long alkyl residues that remarkably enhanced the isomerization activity and the selectivity for di-branched products.[35]

3.3 Dual templating using single, bifunctional surfactants

Dual templating methods were applied in all the examples discussed above, in the sense that two separate structure-directing agents were utilized, each for a different purpose. Ordinary SDAs in the form of molecular amines or ammonium cations were responsible for zeolite micropore formation and secondary, larger templates were used to leave mesopore imprints in the microporous phase. A whole new idea was lately introduced by the group of Ryoo who suggested combining both features within one structure directing agent, thus endowing the template with dual-scale functionality. A number of elegantly designed bifunctional structure directing agents were synthesized, where only one part of the template directs zeolite growth as opposed to the whole molecule. This part consists of an array of quaternary ammonium centers responsible for nucleating the zeolite domains that are held apart by short alkyl linkers, suitable to align the zeolitic entities to form two-dimensionally ordered extended zeolite nanosheets (see Fig. 9). Finally, asymmetric or symmetric decoration of the ammonium centers with longer alkyl chains creates the necessary hydrophobic environment for mesopore formation between the thin zeolite sheets. For instance, when linear gemini-type diquaternary templates with hexamethylene linkers, such as $C_{22}H_{45}$–$N^+(CH_3)_2$–C_6H_{12}–$N^+(CH_3)_2$–C_6H_{13} (here abbreviated as $C_{22}N_2$) were used, very thin MFI zeolite nanosheets formed consisting of only three pentasil layers (about 2 nm).[36] The blue-coded section in Fig. 9 is presumably located with one ammonium center within the zeolite framework, while the second ammonium cation is placed directly at the pore mouth. These nanosheets are separated from each other by the long surfactant tails stacking up either in a multilamellar or a unilamellar fashion, depending on the specific reaction conditions. Calcination proved to result in only small interlamellar mesopores of about 2 nm in the first case unless the sheets were permanently held apart by silica pillars added in a separate step before template removal. The smaller unilamellar sheets collapsed upon calcination in an irregular fashion, thus creating about 15 nm secondary pores in this process.

Based on their modular character it is possible to create numerous different bifunctional templates. The number of cationic centers, the spacer between these centers, the length of the surfactant tails as well as the combination of these different tails on either side of the ammonium cations are variable. It was found that the number of cations has to be at least two in order to generate crystalline zeolite sheets and not non-porous layered silicates. Larger numbers of cations in the molecule can predetermine the thickness of the nanosheets, and the length of the alkyl spacer can lead to different

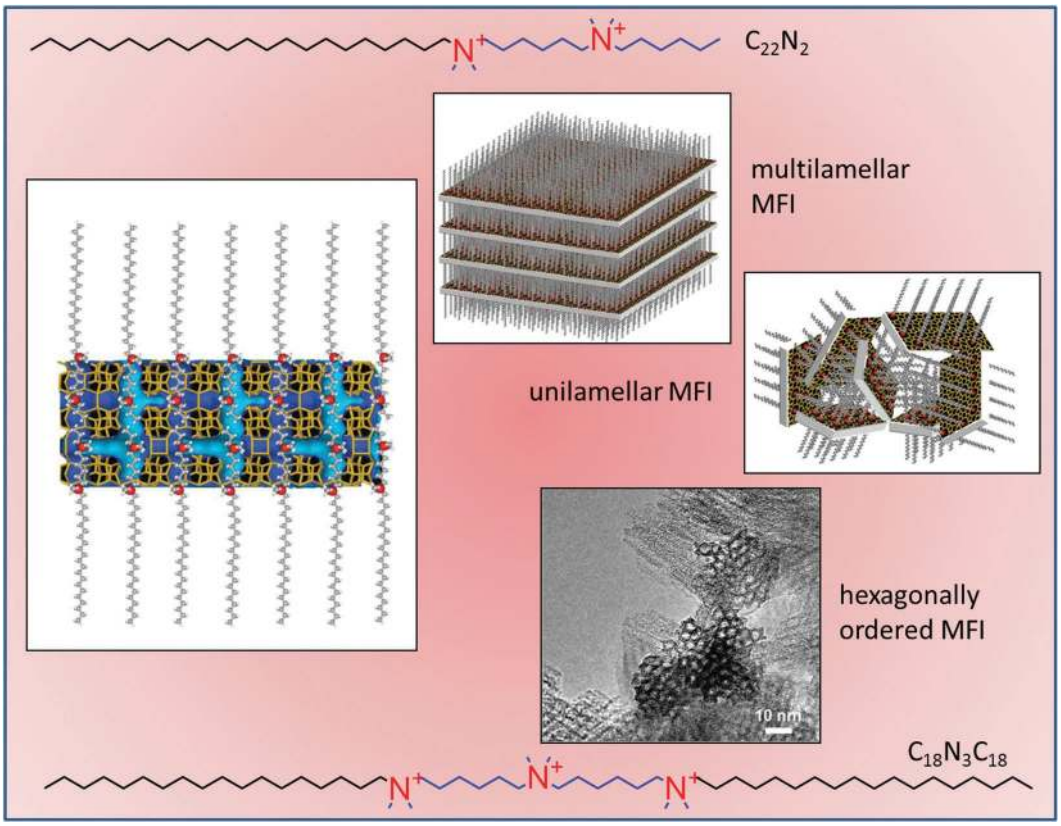

Fig. 9 Representative bifunctional templates and their structure-directing role in MFI nanosheet assembly. Asymmetric bifunctional surfactant molecules with two ammonium centers (top) direct the growth of MFI into ultrathin single nanosheets. Assembly of nanosheets occurs either in multilamellar stacks or disordered unilamellar arrangements, depending on the reaction conditions. Symmetrically constructed bifunctional templates (bottom) can give rise to crystalline, truly hexagonally ordered MFI nanosheets (graphics and TEM reproduced and newly arranged with permission of ref. 36 and 37, copyright Nature 2009 and Science 2011, respectively).

Published on 04 March 2013.

arrangements of the MFI phase, going from multi- to unilamellar. Furthermore, the length of the surfactant tail has an influence on the separation of the nanosheets in the uncalcined samples and should contain between 10 to 22 carbon segments. Shorter tails can induce the growth of nanozeolites. Finally, the alkyl group at the terminal ammonium ion can prevent zeolite growth when it is too voluminous. However, when symmetric bifunctional surfactants with multiple ammonium centers such as 18-N_3-18 ($C_{18}H_{37}$–$N^+(CH_3)_2$–C_6H_{12}–$N^+(CH_3)_2$–C_6H_{12}–$N^+(CH_3)_2$–$C_{18}H_{37}(Br^-)_3$) were used, the first examples of truly hexagonally ordered mesoporous zeolites could be demonstrated.[37] Using this type of templates, 1.7 nm thin MFI zeolite sheets were shaped into cylinders, forming about 3.5 nm mesopores and exposing an extremely large surface of over 1000 $m^2\ g^{-1}$ for potential catalytic reactions (see bottom in Fig. 9). When two or three bridging phenyl groups were added to the center part of the template, a different zeolite type, zeolite beta, was synthesized with these symmetric bifunctional surfactants. However, these products did not feature ordered mesoporosity but consisted of extremely small nanoparticles that generated a very high surface area up to 940 $m^2\ g^{-1}$.

Two-dimensionally ordered zeolite nanosheets with a thickness corresponding to one single unit cell dimension can be regarded as the thinnest zeolite structures possible. Pathways for molecular diffusion are extremely reduced and unusually large surface areas are created. Effectively all acidic centers valuable for catalytic conversion lie exposed on the outside of the zeolite sheet or are in easy reach. Corresponding lamellar zeolites have been described before, the best known member of this group is MCM-22 belonging to the MWW family, but their discovery has mostly relied on serendipity. Bifunctional modular templates as developed by the group of Ryoo seem to offer a much higher level of control for synthesizing hierarchically structured zeolite nanosheets. They constitute a promising toolbox to develop other highly mesoporous zeolites, as long as the special synthetic protocols can be established in an economical way.

The cost-factor associated with this approach can sometimes be reduced as demonstrated recently with two examples. SSZ-13 with CHA topology, a zeolite that is difficult to modify *via* desilication (see Section 5.2) was synthesized in the form of micron-sized mesoporous aggregates by using a typical micropore SDA for the CHA structure (tetramethyl adamantane-hydroxide, TMAdOH) in addition to a bifunctional template $C_{22}H_{45}$–$N^+(CH_3)_2$–$(CH_2)_4$–$N^+(CH_3)_2$–$C_4H_9Br_2$ ($C_{22\text{-}4\text{-}4}$).[38] The expensive bifunctional template was used here only in small amounts sufficient to function as structure-specific spacer

within the outer area of the nanocrystalline particles. In another example, intersecting zeolite nanosheets were made exclusively with the common micropore template tetrabutylphosphonium hydroxide (TBPOH).[39] This SDA is known to stimulate an intergrowth of MFI/MEL zeolites and by choice of the reaction conditions it was exploited for causing a repetitive branching during crystal growth. Even though thin zeolite sheets were created here with a low-cost approach, it might not easily be transferred to other zeolites that do not follow similar growth mechanisms.

4. Bottom-up synthesis of mesoporous zeolites without mesopore template

Constructing mesoporous zeolites might not necessarily need dual templating on the micro- as well as on the mesoscale, as long as the synthesis conditions enable the formation of nanozeolites. The idea is to assemble the nanoparticles into larger, mechanically stable, aggregates with inherent mesoporosity, without needing a secondary template with the associated cost and possible complex synthetic requirements. Here we do not consider nanozeolite powders to be mesoporous zeolites, since their mesopores are only temporarily established when the powder is compacted. To be recognized as truly mesoporous zeolites, mesoporosity should be a permanent, intrinsic materials property (for example, nanozeolites that form colloidal solutions when dispersed in solvents are not considered mesoporous zeolites). Furthermore, nanozeolite powders are generally produced at low yields and their isolation is time-consuming and costly. In contrast, mesoporous zeolites should be made with the least number of reaction steps and preferably with low-cost templates to become potential candidates for industrial application. Considering these points, the self-assembly of nanozeolites into stable mesoporous aggregates seems promising since these materials combine several intriguing aspects: they form an interconnected secondary pore system to ease mass transport and they feature large external surface areas and short intraparticle diffusion pathways. Such stable nanozeolite aggregates can be obtained when either uncommon structure directing agents are applied in the synthesis or even just with common templates but using specific synthesis conditions that favor nanozeolite growth (see Fig. 11).

4.1 Nanozeolite assemblies by cyclic or linear diamino- or diamine structure directing agents

Uncommon, cyclic diammonium templates in place of the usual micropore SDAs were observed by the group of Ryoo to induce an instantaneous gelation with mesoporous structure that crystallized into a zeolite beta replica under hydrothermal conditions. They suggested the term 'pseudomorphic crystallization' for this transformation of zeolite precursor gels into zeolite nanocrystal assemblies since the structural features of the gel were maintained during the process.[40] An explanation for this unusual ability to pre-organize the silica gel is seen in the unique molecular structure of cyclic diammonium cations. When a number of linear and cyclic diammonium or diamine templates were explored, it turned out that zeolite beta (or in some cases MTW, both 12 ring zeolites) was only generated with the cyclic versions while more flexible hexamethylene-linked diammonium cations preferably produced the MFI structure (or in some cases MEL, both 10 ring pentasil zeolites, see Fig. 10). Both types of templates offer a higher local density of ammonium cations than the traditional monoammonium templates, creating a stronger interaction with the negatively charged silica species in the gel. The presence of 5 or 6-ring bridges within the cyclic diammonium templates is a prerequisite for zeolite beta formation (as was found with the bifunctional templates, see Section 3.3). It seems that this geometrical substructure is well suited for 12-ring pore zeolites and that it exerts the necessary rigidity for BEA type zeolites. However, a true pseudomorphic transformation was only observed for zeolite beta with CDM1 and CDM2 (see Fig. 10) while MTW and MFI zeolites crystallize with concomitant compositional changes of the gel. Nevertheless, all zeolites were nanocrystalline assemblies with large mesopore volumes and different mesopore sizes between 5 to 20 nm.

Cost-efficient alternative templates with rigid cyclic geometry include piperidine- or imidazole-based dicationic ionic liquids (DCIL) that were also successfully used for mesoporous beta.[41] A study comparing a variety of different DCILs found that only the chair conformation and not the boat conformation in the piperidine templates is suitable for the formation of zeolite beta. The theoretical and experimental data suggested that the two imidazoles in imidazole-containing templates have to form an angle of 110° to produce mesoporous nanoscale zeolite beta.

4.2 Nanozeolite assemblies by multiple-step pretreatment procedures

High concentrations of zeolite nuclei are necessary to stimulate the growth and assembly of nanozeolites into easily filterable, stable aggregates. We have seen in the preceding section that special templating molecules can induce nanozeolite crystallization, but alternative routes do exist that rely on traditional structure-directing templates for micropore formation. Here, pre-prepared zeolite seeds or seed gels are added at small quantities to the reaction gels to promote the nucleation of the desired phase. This can advantageously suppress any side products and usually results in a significant decrease of reaction times. Ultimately it can even reduce the necessary template concentration to a minimum. However, the reproducibility is highly dependent on the quality of the preformed seeds or gels.

Nanozeolite growth can be stimulated directly when the zeolite precursor gel is itself preconditioned before it is submitted to hydrothermal conversion. Preconditioning can be as simple as aging the aqueous zeolite gel under reflux for a prolonged time or can be quite complex when the synthesis starts from highly diluted ''clear solutions''. Protocols advising multiple reaction steps have been developed for the latter case in order to produce mesoporous ZSM-5 and beta zeolites.[42] Here, water of the zeolite precursor solution is slowly evaporated

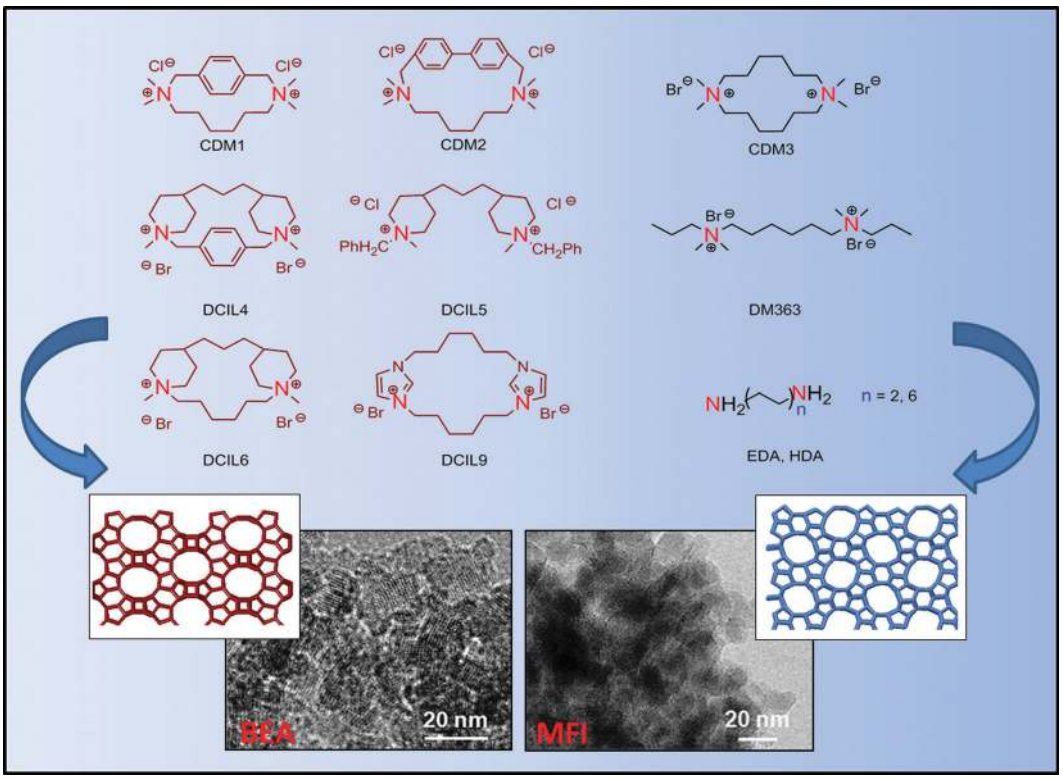

Fig. 10 Overview of diammonium (diamine) templates used as sole structure directing agents. Nanozeolite aggregates of the 12-ring zeolite beta with interstitial mesopores are generated with rigid cyclic diammonium compounds (left) while the corresponding 10-ring MFI structures are obtained with more flexible templates (right). TEM micrographs are reproduced by permission from ref. 40 Copyright (2009) Royal Society of Chemistry.

while the pH is adequately adjusted, and the reaction temperatures and times are varied in order to control the particle size and the resulting mesoporosity. Aggregation was however limited and the particles had to be retrieved *via* centrifugation.

4.3 Nanozeolite assemblies from concentrated gels

Steam-assisted conversion (SAC) is a special method used in zeolite synthesis to prepare zeolites with higher yields, less template or with Si/Al ratios that are otherwise difficult to obtain. Since under these conditions the zeolite precursor mixtures are completely dried before they are converted by steam, the mobility in the reaction mixture is highly reduced compared to common gels. This condition proved helpful against phase separation when secondary templates such as hydrophobic carbons were used to produce mesoporous zeolites. The drying of the precursor gels in the SAC method further implies a maximized local concentration of the reaction partners in the zeolite gel, an ideal condition for massive nucleation. For example, the SAC method was used for the transformation of the amorphous mesoporous silica precursor TUD-1 into nanocrystalline mesoporous ZSM-5 materials.[43] However, several parameters had to be carefully adjusted in this system, such as the drying temperature of the mesoporogen-containing TUD precursor, an induction period had to be observed and the humidity level had to be controlled in order to obtain a high degree of crystallization and mesoporosity.

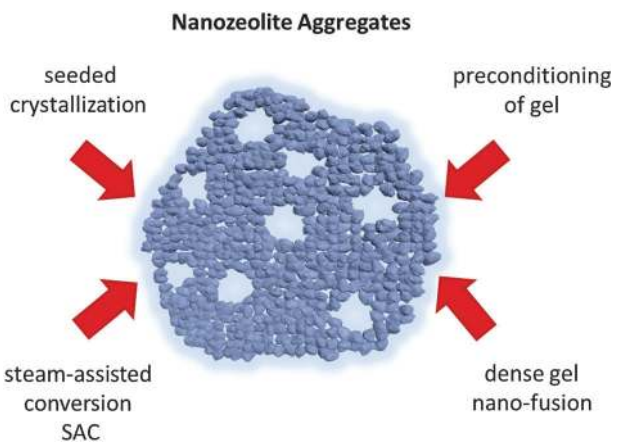

Fig. 11 Synthetic routes to form mesoporous zeolites through nanozeolite assembly.

We could recently show that the SAC method delivers highly mesoporous zeolite beta in one step with nearly 100% yield in very short time without the need for any secondary templates or preformed precursors.[44] Using either commercial mesoporous or colloidal silica sources and the common micropore template TEAOH (tetraethylammonium hydroxide) resulted in 20 nm-sized nanozeolites that assembled into easily retrievable aggregates with defined mesopores of about 13 nm in just 6 hours. A complete conversion into isolated nanocrystals was observed already after 2 hours, but the condensation into an extended

porous network with large mesopore volumes and surface areas required additional 4 hours. This efficient SAC method is applicable to zeolite beta with Si/Al ratios ranging at least from 10 to 30. However, successful conversion requires careful adjustment of the amount of water that is added into the reactor for steam development. It was shown that it has to be scaled with the reactor volume, the mass of the gel and with the reaction temperature.

A quasi-solid-state reaction that is related to the SAC procedure was used to synthesize zeolite materials with pores at three length scales, resulting in macro–meso–microporous (MMM) ZSM-5, TS-1 or beta aggregates.[45] First, a macroporous amorphous titanosilicate was assembled by the spontaneous reaction of titanium isopropoxide (for TS-1) and tetramethyl orthosilicate (TMOS). This dry matrix was then impregnated with a silica solution containing the micropore template, dried and finally converted at 130 °C in a glycerol medium. The amorphous walls defining the 1 μm macropores were transformed into 200 nm TS-1 nanoparticles with 4.7 nm interparticle mesopores, resulting in a hierarchical TS-1 material with nearly twice the surface area (580 $m^2\ g^{-1}$) as TS-1 nanoparticles prepared as reference.

Even though the SAC method creates excellent mesoporous zeolites as discussed above, it requires careful tuning of the reaction conditions, which can create issues when upscaling is desired. This method also reduces the potential reactor volume because it has to be partitioned in order to separate the dry gel from the water for steam production. In an effort to simplify this process we have used highly concentrated gels in a hydrothermal conversion to stimulate nucleation of nanozeolites.[46] Dense zeolite precursor gels with $SiO_2 : H_2O$ ratios of only about 1 : 6 were prepared using comparable amounts of water as those needed for a SAC process. The gels contained aluminum sulfate as potential nucleation promoter and were crystallized in conventional reactors at fairly high temperatures corresponding to those during SAC treatment. Strikingly, highly mesoporous zeolite beta aggregates were formed in short times (4 to 6 hours) following this approach. Translucent nanozeolite gels were obtained that turn into colloidal suspensions of individual nanocrystals when dispersed in water. However, when these gels are dried and are directly calcined for template removal they undergo a partial condensation/aggregation that was named 'nanofusion', thus generating self-sustained mesoporous nanozeolite aggregates. The mesopore size is tunable by simply changing the reaction time. With prolonged time, crystallites increasingly condense into larger domains, thus creating interstitial pores of larger sizes ranging from 15 to 35 nm when the reaction time is extended from 6 to 72 hours. Acidic mesoporous zeolite beta can directly be made in this one-step process when sodium-free synthesis gels are used.

Usually, nanozeolites are prepared from highly diluted "clear-solution" precursor mixtures and a significant number of nanozeolite phases are known today, including ZSM-5, beta, FAU, LTA ad LTL. These and possibly even other structures may well be suitable candidates to extend the above dense gel/fusion approach towards additional mesoporous zeolites.

5 Mesoporosity through etching of premade zeolites

In contrast to the methods described in the previous sections, it is also possible to create mesopores in zeolites in a secondary reaction, that is, after the microporous zeolites are synthesized and freed from micropore templates through calcination. Special dealumination or desilication leaching procedures may be used to create amorphous areas in the zeolite framework, which will constitute the mesopores upon extraction of the amorphous debris. Principally, leaching describes a destructive process intended to sacrifice part of the typical micron-sized zeolite crystals for creating larger external surfaces in the form of mesopores. An informative critical review that assesses these leaching procedures as well as the already described bottom-up strategies with a view of industrial application has recently been published.[6b]

5.1 Mesopores through dealumination

Selective dealumination has been performed for decades since it was found that preparing zeolites with a higher Si/Al ratio is beneficial for their stability and that it creates acid sites of higher strength. Removing alumina species from the framework may already occur during calcination when the conditions are harsh and the specific zeolite type is less stable. Defect sites are formed through hydrolysis of the Si–O–Al bonds, thus leaving extra-framework alumina species behind. The severity of this process can be increased when extra steam is added, a process that has been used for many years for dealuminating zeolite Y. Condensation of the defect sites then creates the ultrastable zeolite Y with a higher Si/Al ratio (USY) that is predominantly used as cracking catalyst in FCC (fluidized catalytic cracking) processing. Extracting the amorphous alumina residues by a mild acid wash with diluted nitric acid or the complexing oxalic acid finally frees up cavities or pores with broad size-distributions between about 2 and 50 nm.

Dealumination is not restricted to zeolite Y but has also been applied to mordenite, beta and ferrierite, mostly by direct leaching with more concentrated acids, that is, the mesopores are not created by hydrolysis from steam but by direct attack of the acid. Acids of different strength such as acetic, oxalic, tartaric acid or nitric, sulfuric or hydrochloric acid were used at different concentrations (even 6 M HCl), providing results that are highly dependent on the nature of the zeolite. For instance, in a comparative study of three different structures, zeolite beta was easier to dealuminate than mordenite, while ZSM-5 was nearly unaffected under similar conditions. At the same time, dealumination of zeolite beta led to excessive loss of crystallinity, while the mesopore volume increased markedly only for mordenite.[47] Generally, extraction of aluminum from the zeolite framework necessarily leads to a change in Si/Al ratio, and hence the acidity, while mesopores are formed simultaneously. Understanding the impact of mesoporosity on changes in catalytic activity can become difficult under these circumstances. This complication may be one reason that mesopore formation through leaching has been lately

performed by desilication instead. Silica is usually present at higher abundance than aluminum in the zeolite and changes in the Si/Al ratio are not as drastic upon desilication, especially since under some circumstances both framework elements are dislodged from the framework together (see Section 5.2). Furthermore it was found that the steam-created mesopore volume in USY is largely based on isolated cavities rather than on interconnected mesopores and thus could not support enhanced diffusion of large molecules.[48] Enabling just that, an interconnected pore system on the mesoscale is the goal of the top-down desilication route.

5.2 Mesopores through desilication

The accumulated knowledge about desilication was recently summarized by Verboekend *et al.* who have performed extensive research in this field.[49] We refer the readers to this review and the literature cited within for a more detailed account on this approach. Since the preferential removal of silica is the goal here, bases are used for the post-synthetic treatment of typical micron-sized zeolite crystals. The group of Matsukata has clearly shown by SEM how a treatment with NaOH changes the morphology of single-crystal ZSM-5 from a smooth into a jagged surface, thus creating large mesopore volumes without seemingly altering its X-ray crystallinity.[50] However, about 40% of the silicon was dissolved from the zeolite. Since then a large number of publications have described the effects of desilication on mainly ZSM-5 and other MFI-type zeolites and to a lesser extent on the zeolites beta, faujasite, ferrierite, chabasite, TUN and some one-dimensional zeolites like mordenite, ZSM-22, ZSM-12, ITQ-4 and SSZ-35 (for a comprehensive overview please refer to ref. 8). Many of the published procedures rely on a one-step treatment with NaOH of the respective calcined zeolites, usually at low base concentration (0.2 M NaOH), slightly elevated temperature (25–80 °C) and times between 30 minutes to several hours. The extent of dissolution and creation of the mesopore volume is determined by the length and intensity of the treatment. It was soon realized that the extraction of silica was limited to a certain Si/Al ratio, ranging from 25 to 50 in ZSM-5. At lower values the negatively charged AlO_4^--tetrahedra were found to prevent the extraction, while in silica-rich samples uncontrolled excessive Si-extraction led to wide pore-size distributions and extremely low yields through massive zeolite dissolution. Observations on Al-zoned ZSM-5, where the Al-rich rim was much less destroyed than the interior of the zeolites, suggested that the extraction of silica is the predominant process under base leaching. Due to the important role of the aluminum species in the dissolution mechanism, they are viewed as 'pore-directing' species. Nevertheless, even with zeolites having a medium Si/Al-ratio, base leaching creates mesopores usually accompanied by a loss of micropore volume and overall yield, and conditions have to be optimized carefully for each zeolite.

In order to limit the destructive effect of the leaching process, alternative reagents such as sodium aluminate have been evaluated. It was found that in this way the dissolution could be better controlled, likely caused by a protective aluminum hydroxide deposit on the zeolite surface. Consequently, when this amorphous layer was dissolved by an additional acidic wash, a high mesoporosity with smaller mesopores and an overall larger yield was obtained. It turned out that a similar mechanism is at play when low Si/Al ZSM-5 is extracted with NaOH: the dislodged alumina forms an amorphous layer at the pore mouths, decreasing microporosity, which can be restored by a subsequent HCl wash. This acid wash simultaneously regenerates the Si/Al ratio close to the original value by removing the Lewis-acidic alumina species. The accessible Si/Al range for leaching procedures could be further extended to silica-rich samples by exploiting a similar mechanism. For instance, mesoporous silicalite was formed when metal hydroxides such as $Al(OH)_4^-$, $Ga(OH)_4^-$ or ammonium hydroxides such as tetramethyl- or tetrapropyl-ammonium hydroxide were added to the basic extraction solution. These agents seem to function as protectors against dissolution, either through reinsertion of the metals into the created defect sites or in the case of the alkylammonium hydroxides through surface adhesion caused by the high adsorption affinity towards the zeolite surface.[51] "Pore-directing agents" (PDA) is the descriptive reference for these additives in some reports. With this more fine-tuned approach of desilication it is now possible to extend the Si/Al range from about 12 to 1000.

However, the Si/Al ratio is not the only property that has a strong influence on the outcome during desilication. The morphology of the original zeolites, either consisting of large single crystals or of intergrown smaller particles with larger external surface area, naturally influences any dissolution process. Grain boundaries and defects in the latter add to the fact that they are much more susceptible to etching which occurs predominantly along those locations. Furthermore, even though desilication was applied to a number of other structure types besides ZSM-5, it needed careful adaptation of the general procedure for each different zeolite and sometimes even for each composition of the same zeolite type. For instance, it was shown for a variety of faujasite zeolites that both the Si/Al ratio and the pretreatment conditions (steaming, dealumination) required each a different procedure.[52] Al-rich samples (Si/Al about 2.5) needed a mild dealumination pretreatment (to Si/Al > 4) with chelating acids such as H_4EDTA prior to the desilication step in order to achieve any mesopore formation, while the Si/Al range between 4–6 required a mild acid wash after desilication (with Na_2H_2EDTA) to remove the abundantly formed Al-debris. On the other hand, severely steamed and high silica Y had to be treated with additional pore-growth moderators in the basic solution to prevent massive amorphization. A high mesopore or external surface area of 258 $m^2\ g^{-1}$ (22 $m^2\ g^{-1}$ in the parent zeolite) was created in this example, however with an overall yield of only 54% and a crystallinity of 35% due the severe treatment conditions.

Amorphization with severe dissolution and often some loss in micropore volume are side effects frequently observed when using the desilication route. Furthermore, highly siliceous zeolites or zeolites that contain Al in strained four-ring building units such as faujasite, chabasite or beta easily experience a

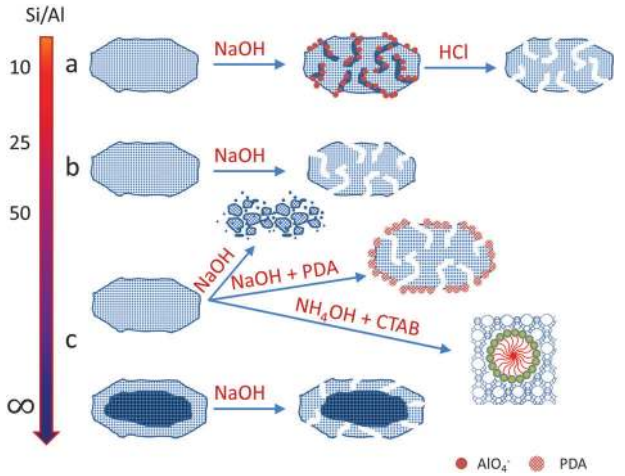

Fig. 12 Summary of desilication procedures used for different Si/Al ranges. (a) Low Si/Al ratio: dislodged AlO_4^--tetrahedra reassemble at the zeolite mesopore surfaces and prevent further dissolution. Mesopores are blocked until a secondary acid wash is performed. (b) Medium Si/Al ratio: a one-step standard desilication is possible (0.2 M NaOH, 30 min, 65 °C). (c) High Si/Al ratio (or less stable topologies): standard conditions result in excessive dissolution; alternative treatments include the (I) use of milder bases, (II) the addition of pore-directing agents (PDA), (III) a recrystallization with surfactants, (IV) partial detemplation: the micropore template (dark blue area) is only partially removed prior to desilication.

loss in crystallinity by this method. To alleviate these problems, yet another variation of desilication proved to be helpful as shown in a study on zeolite beta. Here, desilication was performed on only lightly calcined and thus partially detemplated zeolites. Residual template molecules within the micropores effectively shielded the framework from base attack and the desilication strength could be tailored by the calcination temperature and duration.[53] However, extra-large zeolite beta crystals had to be synthesized *via* the fluoride-route for this purpose.

A surfactant-based desilication technique was developed to obtain a better control over the mesostructuring process irrespective of the type and Si/Al ratio of the zeolite. Many attempts have been made combining surfactants with NaOH solutions for desilication that have ultimately resulted in partial zeolite transformation into zeolite/mesoporous oxide composites. But when FAU, MOR or MFI zeolites were treated at 150 °C with a mildly basic solution of NH_4OH containing cetyltrimethyl ammonium bromide (CTAB), mesoporous Y zeolite was recrystallized with a recovery near 100% and nearly no loss in micropore volume.[54] Even tuning of the mesopores between 2.5 and 4.5 nm was achieved by choosing surfactants with increasing chain length. It is suggested that the negatively charged defect sites created by the crystal dissolution are neutralized by electrostatic interactions with the positively charged surfactant molecules, which slowly induce an *in situ* surfactant-assisted recrystallization. For an overview of the different desilication methods see Fig. 12.

In summary, the desilication route represents one of the most popular methods for mesopore formation and has been explored for a number of zeolite structures. Care has to be taken especially regarding the concentration of the base solution, since more robust structures such as FER and MOR require harsher conditions that are detrimental for less stable structures such as CHA, BEA or MWW. Final yields and mesopore sizes vary accordingly. However, adjustments of the reaction conditions and the appropriate choice of additives enable the application of this method over a wide range of zeolites and framework compositions.

Comparison of structural parameters of mesoporous MFI zeolites prepared by different routes. Since mesoporous MFI type zeolites have been prepared by nearly all methods presented above, we have included a table that compares the structural properties of some representative samples with those of conventional microporous ZSM-5. It can be seen that carbon black pearls and polymers tend to result in mesopores of larger sizes with broader pore size distributions. The total surface area is relatively close to that of the parent compound when hard templating is used, it is often lower when leaching procedures are applied, and is impressively large in some instances when silylating agents or bifunctional templates direct the mesopore formation. This is mainly due to the different morphologies of the resulting zeolites, where the single crystals differ markedly from the nanozeolite aggregates. Another important aspect is the diameter of the newly formed mesopores, being more defined and on a smaller scale when molecular templates are being used, which in some instances even allows for tuning the pore size (Table 1).

6. Mesoporous zeolites and catalysis

Exploring the potential of synthesizing mesoporous zeolites was mainly stimulated by the promise of an extended and more efficient use of zeolites in catalysis. While synthetic aspects still dominate the majority of publications in this field, there is lately an increased effort to compare the reactivity of the newly made mesoporous zeolites with the reactivity of their microporous "parent" materials. Evaluated are either model reactions or reactions that typically encounter mass transport limitations in the native zeolites. In these studies, mesoporous zeolites usually come out as winners, since their catalytic activities are generally higher or the lifetime of the catalysts is longer, both factors often caused by improved diffusion and access to active sites. However, care has to be taken when the selectivity of a reaction is compared since the acidic properties of the parent and the mesoporous sample can vary drastically. Especially, leaching methods tend to change the Si/Al distribution during mesopore formation and even Lewis sites may be newly formed in the process. This complicates a true cause–effect interpretation of the catalytic data and stresses the need for extensive materials characterization. Here we can only mention a few selected classes of catalytic reactions examined with mesoporous zeolites, and the reader is referred to the excellent review by Holm *et al.* where these examples are discussed in more detail.[55]

Alkylation reactions of benzene with ethylene or propene seem to benefit from mesopores in showing a higher activity as well as selectivity towards the monoalkylated products, while in

Table 1 Physical properties of mesoporous MFI-type zeolites prepared by different synthesis routes in comparison to typical values for conventional microporous ZSM-5

Ref.	Year	Si/Al	Mesopore-template	Mesopore size (nm)	Micropore volume (ml g^{-1})	Mesopore volume (ml g^{-1})	Surface area (m^2 g^{-1})	Morphology*
49		39	None; parent MFI	—	0.17	0	316	
			Hard					
8	2000	—	BP 2000	5–50	0.09	1.01		Sxtl
11	2003	—	Carbon aerogel	11	0.15	0.2	385	Monolith
13	2012	SIL	Graphene sheets	2	0.10	0.016	359	Sxtl
14	2012	SIL	CMK	8.7	0.14	0.17	350	Poly
15	2008	SIL	3Dom	6	0.14	0.99	495	Poly
17	2007	—	Sucrose/SiO_2	10, tunable to 20	0.14	0.08	359	Poly
			Soft					
19	2012	37	Copolymer	10–60	0.08	0.31	365	Sxtl
24	2006	20	Organosilane surfactants C_{12}–C_{18}	2.1, tunable to 7.4	—	—	590	Poly
26	2008	17	TPDAC	15	—	0.7 (total)	570	Poly
30	2006	45	PHAPTMS	5	0.12	314 ext. surf. area	586	Poly
31	2011	41	PHAPTMS + propanol	2–6	0.15	0.52	719	Poly
33	2008	26	PTES	3–8	0.12	0.31	526	Poly
35	2009	30–∞	C_{22}–N_2	15	—	—	710	Unilamellar
36	2011	15	18-N_3-18	3.5	—	1.58 (total)	1190	Ordered mesopores
39	2009	55–∞	Monotemplated CDM3	*Ca.* 5	0.12	0.48	549	Poly
			Leach					
49	2000	39	NaOH	4	0.13	0.28	320 (yield 60–70%)	Sxtl
50	2011	1320	Base + PDA	10 (broad)	0.13	0.32	568 (yield 60–70%)	Sxtl

*Sxtl = single crystal, Poly = polycrystalline aggregates.

diffusion-limited ZSM-5 or MOR zeolites polyalkylation is more dominant. Even the alkylation with benzylalcohol was dramatically enhanced with mesoporous zeolites of this type. Methanol to hydrocarbon or to gasoline (MTH or MTG) conversions showed longer lifetimes with ZSM-5 that were explained with a lower propensity for coke formation, which formed predominantly on the external surface *versus* the internal micropores. When ZSM-5 sheets made with bifunctional templates were tested by the Ryoo group for cracking high-density polyethylene, they found a substantially improved cracking activity, presumably due to the ease of accessing the acid sites. However, the shape selectivity known from purely microporous MFI was lost in these extremely thin crystalline domains.[36] Isomerization of fatty acids (C_{18}) profited greatly from an increase in external surface area in zeolite beta, where the internal surface was out of reach for these large molecules. Catalytic cracking is one of the most important applications of zeolites and it is shown in the above-mentioned review that for the cracking of small substrates (C_8) there is no benefit derived from secondary pores; however, with larger substrates generally a higher activity is found. Mesopores are especially important when condensation reactions are considered. Microporous zeolites are usually too restricted in their pore sizes to process larger reaction products but when silylated surfactants were used as shown in Fig. 6 to create highly mesoporous ZSM-5, it was possible to boost the catalytic activity for forming jasminaldehyde from 3.9 to 98%.[25]

7. Summary of achievements and challenges

Today, the benefits of a secondary larger pore system in the microporous zeolites are established by an impressive number of publications covering diverse applications in catalysis such as alkylation, isomerization, cracking or condensation reactions.[55] Many inventive synthetic approaches such as those discussed above have shown that almost all important zeolites as well as zeotype structures can be endowed with mesopores. However, when an industrial realization is envisioned, several aspects need to be considered. First of all, the highly desirable properties of microporous zeolites, namely their selectivity based on microporosity, their stability due to their crystallinity as well as their defined acidity resulting from a fairly homogenous distribution of aluminum sites in the crystalline lattice should not be compromised when a second pore system is implemented. These properties set zeolites apart from the many other mesoporous materials that are already available through different synthesis routes. Furthermore, synthetic protocols should be cost-effective and should involve few reaction and processing steps to make an industrial implementation realistic. To keep a potential application as broad as possible with a specific zeolite structure, mesoporous zeolites would benefit from the tunability of their mesopore system, thus allowing a facile adjustment of pore-size, pore volume and mesopore surface area. Not all of these requirements can likely be met by one specific method, hence making the diversity of the developed synthetic protocols so attractive. The desilication approach has advanced probably the most regarding scalability and applicability. It was initially focused mainly on MFI type zeolites but now covers the widest range of zeolite structures such as MOR, BEA, FAU, CHA, MTW, FER, TON, IFR, STF and even the zero-dimensional AST. This top-down method appears to be straightforward to use, but the degenerative process can induce loss of crystallinity, and usually involves a reduction of microporosity and overall yield and changes in chemical properties through a change in Si/Al ratio need to be carefully addressed.

For multiple-step methods such as carbon-replication the cost factor might turn out to be prohibitive, but the final materials could provide highly ordered model systems for addressing fundamental questions of transport and catalysis in porous materials. On the other hand, specialized structure-specific templating molecules such as bifunctional surfactants show promise to provide access to additional new, high-surface zeolite structures offering the ultimate in short diffusion pathways. Silylating agents appear to be a versatile route to create many zeolite structures with tunable mesoporosity, while the nano-fusion approach offers a very effective method relying on the ability to form nanozeolites in highly concentrated gels. Zeolite chemistry is quite complex and implementing mesoporosity might bring about changes in other zeolite properties that need to be carefully studied before catalytic data are evaluated and fully understood. As we have shown in this review, numerous complementary methods have been developed to create mesoporous zeolites with different properties – this powerful toolbox can now be used to further extend the great potential of zeolites to many new and promising applications in catalysis.

Acknowledgements

Financial support through BASF SE (Germany) is gratefully acknowledged. We thank Bastian Rühle for generating the graphics design in the TOC as well as in Fig. 1.

References

1 http://www.iza-structure.org/databases/.
2 J. Jiang, J. Yu and A. Corma, *Angew. Chem., Int. Ed.*, 2010, **49**, 3120–3145.
3 J. Jiang, J. L. Jorda, J. Yu, L. A. Baumes, E. Mugnaioli, M. J. Diaz-Cabanas, U. Kolb and A. Corma, *Science*, 2011, **333**, 1131–1134.
4 V. Meynen, P. Cool and E. F. Vansant, *Microporous Mesoporous Mater.*, 2007, **104**, 26–38.
5 S. Mintova and J. Cejka, in *Introduction to Zeolite Science and Practice, 3rd Revised Edition. [In: Stud. Surf. Sci. Catal.]*, ed. Cejka Jiri, H. van Bekkum, A. Corma and F. Schüth, 2007, vol. 168, pp. 301–326.
6 (*a*) Y. Tao, H. Kanoh, L. Abrams and K. Kaneko, *Chem. Rev.*, 2006, **106**, 896–910; (*b*) R. Chal, C. Gérardin, M. Bulut and S. van Donk, *ChemCatChem*, 2011, **3**, 67–81; (*c*) J. Perez-Ramirez, C. H. Christensen, K. Egeblad, C. H. Christensen and J. C. Groen, *Chem. Soc. Rev.*, 2008, **37**, 2530–2542.
7 L.-H. Chen, X.-Y. Li, J. C. Rooke, Y.-H. Zhang, X.-Y. Yang, Y. Tang, F.-S. Xiao and B.-L. Su, *J. Mater. Chem.*, 2012, **22**, 17381–17403.
8 K. Möller and T. Bein, in *Comprehensive Inorganic Chemistry II*, ed. R. Schlögl, Elsevier, 2013, vol. 7.16, in press.
9 C. J. H. Jacobsen, C. Madsen, J. Houzvicka, I. Schmidt and A. Carlsson, *J. Am. Chem. Soc.*, 2000, **122**, 7116–7117.
10 M. Y. Kustova, P. Hasselriis, C. H. Christensen and C. Hviid, *Catal. Lett.*, 2004, **96**, 205.
11 K. Egeblad, M. Kustova, S. K. Klitgaard, K. Zhu and C. H. Christensen, *Microporous Mesoporous Mater.*, 2007, **101**, 214–223.
12 Y. Tao, H. Kanoh and K. Kaneko, *J. Am. Chem. Soc.*, 2003, **125**, 6044–6045.
13 I. Schmidt, A. Boisen, E. Gustavsson, K. Stahl, S. Pehrson, S. Dahl, A. Carlsson and C. J. H. Jacobsen, *Chem. Mater.*, 2001, **13**, 4416–4418.
14 D. Li, L. Qiu, K. Wang, Y. Zeng, D. Li, T. Williams, Y. Huang, M. Tsapatsis and H. Wang, *Chem. Commun.*, 2012, **48**, 2249–2251.
15 H. S. Cho and R. Ryoo, *Microporous Mesoporous Mater.*, 2012, **151**, 107–112.
16 W. Fan, M. A. Snyder, S. Kumar, P.-S. Lee, W. C. Yoo, A. V. McCormick, R. Lee Penn, A. Stein and M. Tsapatsis, *Nat. Mater.*, 2008, **7**, 984–991.
17 H. Chen, J. Wydra, X. Zhang, P.-S. Lee, Z. Wang, W. Fan and M. Tsapatsis, *J. Am. Chem. Soc.*, 2011, **133**, 12390–12393.
18 M. Kustova, K. Egeblad, K. Zhu and C. H. Christensen, *Chem. Mater.*, 2007, **19**, 2915–2917.
19 F.-S. Xiao, L. Wang, C. Yin, K. Lin, Y. Di, J. Li, R. Xu, D. S. Su, R. Schlögl, T. Yokoi and T. Tatsumi, *Angew. Chem., Int. Ed.*, 2006, **45**, 3090–3093.
20 F. Liu, T. Willhammar, L. Wang, L. Zhu, Q. Sun, X. Meng, W. Carrillo-Cabrera, X. Zou and F.-S. Xiao, *J. Am. Chem. Soc.*, 2012, **134**, 4557–4560.
21 K. Möller, B. Yilmaz, U. Müller and T. Bein, *Chem. Mater.*, 2011, **23**, 4301–4310.
22 Y. Zhu, Z. Hua, J. Zhou, L. Wang, J. Zhao, Y. Gong, W. Wu, M. Ruan and J. Shi, *Chem.–Eur. J.*, 2011, **17**, 14618–14627.
23 H. Tao, C. Li, J. Ren, Y. Wang and G. Lu, *J. Solid State Chem.*, 2011, **184**, 1820–1827.
24 H. Wang and T. J. Pinnavaia, *Angew. Chem., Int. Ed.*, 2006, **45**, 7603–7606.
25 M. Choi, H. S. Cho, R. Srivastava, C. Venkatesan, D.-H. Choi and R. Ryoo, *Nat. Mater.*, 2006, **5**, 718–723.
26 A. Inayat, I. Knoke, E. Spiecker and W. Schwieger, *Angew. Chem., Int. Ed.*, 2012, **51**, 1962–1965.
27 V. N. Shetti, J. Kim, R. Srivastava, M. Choi and R. Ryoo, *J. Catal.*, 2008, **254**, 296–303.
28 H. Xin, A. Koekkoek, Q. Yang, R. van Santen, C. Li and E. J. M. Hensen, *Chem. Commun.*, 2009, 7590–7592.
29 D. H. Lee, M. Choi, B. W. Yu and R. Ryoo, *Chem. Commun.*, 2009, 74–76.
30 K. Cho, H. S. Cho, L.-C. de Menorval and R. Ryoo, *Chem. Mater.*, 2009, **21**, 5664–5673.
31 D. P. Serrano, J. Aguado, J. M. Escola, J. M. Rodriguez and A. Peral, *Chem. Mater.*, 2006, **18**, 2462–2464.
32 D. P. Serrano, J. Aguado, J. M. Escola, A. Peral, G. Morales and E. Abella, *Catal. Today*, 2011, **168**, 86–95.
33 D. P. Serrano, J. Aguado, G. Morales, J. M. Rodriguez, A. Peral, M. Thommes, J. D. Epping and B. F. Chmelka, *Chem. Mater.*, 2009, **21**, 641–654.
34 R. Srivastava, N. Iwasa, S.-i. Fujita and M. Arai, *Chem.–Eur. J.*, 2008, **14**, 9507–9511.
35 Y. Fan, H. Xiao, G. Shi, H. Liu and X. Bao, *J. Catal.*, 2012, **285**, 251–259.

36 M. Choi, K. Na, J. Kim, Y. Sakamoto, O. Terasaki and R. Ryoo, *Nature*, 2009, **461**, 246–249.
37 K. Na, C. Jo, J. Kim, K. Cho, J. Jung, Y. Seo, R. J. Messinger, B. F. Chmelka and R. Ryoo, *Science*, 2011, **333**, 328–332.
38 L. Wu, V. Degirmenci, P. C. M. M. Magusin, B. M. Szyja and E. J. M. Hensen, *Chem. Commun.*, 2012, **48**, 9492–9494.
39 X. Zhang, D. Liu, D. Xu, S. Asahina, K. A. Cychosz, K. V. Agrawal, Y. Al Wahedi, A. Bhan, S. Al Hashimi, O. Terasaki, M. Thommes and M. Tsapatsis, *Science*, 2012, **336**, 1684–1687.
40 K. Na, M. Choi and R. Ryoo, *J. Mater. Chem.*, 2009, **19**, 6713–6719.
41 R. Kore, B. Satpati and R. Srivastava, *Chem.–Eur. J.*, 2011, **17**, 14360–14365.
42 A. Petushkov, G. Merilis and S. C. Larsen, *Microporous Mesoporous Mater.*, 2011, **143**, 97–103.
43 J. Zhou, Z. Hua, J. Zhao, Z. Gao, S. Zeng and J. Shi, *J. Mater. Chem.*, 2010, **20**, 6764–6771.
44 K. Möller, B. Yilmaz, R. M. Jacubinas, U. Müller and T. Bein, *J. Am. Chem. Soc.*, 2011, **133**, 5284–5295.
45 L.-H. Chen, X.-Y. Li, G. Tian, Y. Li, J. C. Rooke, G.-S. Zhu, S.-L. Qiu, X.-Y. Yang and B.-L. Su, *Angew. Chem., Int. Ed.*, 2011, **50**, 11156–11161.
46 K. Möller, B. Yilmaz, U. Müller and T. Bein, *Chem.–Eur. J.*, 2012, **18**, 7671–7674.
47 M. D. González, Y. Cesteros and P. Salagre, *Microporous Mesoporous Mater.*, 2011, **144**, 162–170.
48 P. Kortunov, S. Vasenkov, J. Kärger, R. Valiullin, P. Gottschalk, M. Fé Elía, M. Perez, M. Stöcker, B. Drescher, G. McElhiney, C. Berger, R. Gläser and J. Weitkamp, *J. Am. Chem. Soc.*, 2005, **127**, 13055–13059.
49 D. Verboekend and J. Perez-Ramirez, *Catal. Sci. Technol.*, 2011, **1**, 879–890.
50 M. Ogura, S.-Y. Shinomiya, J. Tateno, Y. Nara, E. Kikuchi and M. Matsukata, *Chem. Lett.*, 2000, 882–883.
51 D. Verboekend and J. Pérez-Ramírez, *Chem.–Eur. J.*, 2011, **17**, 1137–1147.
52 D. Verboekend, G. Vile and J. Perez-Ramirez, *Adv. Funct. Mater.*, 2012, **22**, 916–928.
53 J. Perez-Ramirez, S. Abello, A. Bonilla and J. C. Groen, *Adv. Funct. Mater.*, 2009, **19**, 164–172.
54 J. Garcia-Martinez, M. Johnson, J. Valla, K. Li and J. Y. Ying, *Catal. Sci. Technol.*, 2012, **2**, 987–994.
55 M. S. Holm, E. Taarning, K. Egeblad and C. H. Christensen, *Catal. Today*, 2011, **168**, 3–16.